Available online at www.sciencedirect.com
ScienceDirect
Catalysis Today 119 (2007) 13–18
CATALYSIS TODAY
www.elsevier.com/locate/cattod

Characterization and activity of Mo supported catalysts for diesel deep hydrodesulphurization

Aijun Duan [a,*], Guofu Wan [a], Zhen Zhao [a], Chunming Xu [a], Yanying Zheng [b], Ying Zhang [b], Tao Dou [b], Xiaojun Bao [b], Keng Chung [c]

[a] State Key Laboratory of Heavy Oil Processing, China University of Petroleum, Beijing 102249, PR China
[b] Key Laboratory of Catalysis, China University of Petroleum, Beijing 102249, PR China
[c] Syncrude Canada Ltd., 9421-17 Avenue, Edmonton, Alberta T6N 1H4, Canada

Available online 8 September 2006

Abstract

Various highly dispersed Mo supported catalysts with various carriers were prepared for deep hydrodesulphurization of diesel. The carriers included a high surface area and large pore volume γ-Al_2O_3, two types of meso-microporous composite molecular sieves prepared by incipient-wetness impregnation method. A new mesoporous $MoSiO_x$ catalyst synthesized with in situ composite method was also studied. The hydrodesulphurization experiments were carried out in a micro-reactor over different catalysts including Mo supported series and a commercial catalyst. Spectroscopic techniques (FT-IR and UV–vis DRS) were utilized to determine the structure of MoO_x species. The catalyst characterizations of BET, XRD, FT-IR, UV–vis DRS and FTIR pyridine adsorption indicated that the existences of metal active component of Mo in the catalysts were highly dispersed nano MoO_3 clusters and the Mo series catalysts had high surface areas and plenty of large pores which were propitious to the diffusions of reactant and product molecules. Cat_{NiMo} exhibited the highest *B*/*L* acidity ratio and higher total concentration of Brønsted acid sites and Lewis acid sites, and its HDS activity also gave the highest in this study to produce a sulphur-free diesel, which was verified by the sulphur content in products analyzed by GC–MS methods.

Keywords: Hydrodesulphurization; Molybdenum and nickel catalyst; Ultra low sulphur diesel; Mesoporous materials

1. Introduction

Recently the stringent environmental regulations established high quality transportation fuel specification to reduce automobile emissions and to minimize the environmental pollution, e.g. the sulphur content in diesel is required to be lowered to or less than 50 ppm in America, in European countries the sulphur in diesel less than 10 ppm S has been implemented since 2005. To meet this assignment, it has been paid more attentions in product upgrading via deep or ultra deep hydrodesulphurization (HDS) of diesel [1,2].

It is well known that alkyl substituted dibenzothiophenes (DBT) are the most refractory sulphur compounds in light oil for HDS. Transitional metal sulphides (TMS) hydroprocessing catalysts have been widely used for 70 years. Metal sulphides from group VI (Mo, W) promoted by sulphides of group VIII (Co, Ni), generally supported on alumina, are the most economical TMS which have high activity, selectivity and stability for heteroatom removal and product refining [3,4]. The active phase on these hydroprocessing catalysts has a Ni(Co)Mo(W)S-like structure, and active sites are located at edge surfaces of the $Mo(W)S_2$ [5,6].

One of the important factors that affect the efficiency of a hydrodesulphurization catalyst is the interaction between the active phases and the support. Metal–support interactions influence not only the dispersion of the active components, but also their reducibility and sulphidability, e.g. modification of the morphology of the sulphide active phase, interactions of chemical environment of acid sites. The development of new supports for hydrotreatment catalysts have been very active urged by the stringent regulations concerning the restricted level of sulphur admitted in fuels. Some results have been summarized in reviews and open literatures concerning hydrotreatment catalyst and deep hydrodesulphurization

* Corresponding author. Fax: +86 10 89731586.
E-mail address: duanaijun@cup.edu.cn (A. Duan).

0920-5861/$ – see front matter © 2006 Elsevier B.V. All rights reserved.
doi:10.1016/j.cattod.2006.08.049

[7–10]. The typical specific surface area of such tranditional oxide supports before 1991 remained below 100 m^2/g (after calcination at 773 K), and the porosity were also not adapted for hydrotreating applications. Many improvements of new type support preparation, resulted in higher specific surface area and larger pore diameters, were obtained in the past decade.

Many supports were used in hydrotreating catalyst as carbon, simple oxides (TiO_2, ZrO_2), binary oxides, acidic materials and clays [11]. For instance, mixed oxide supports include TiO_2–ZnO, TiO_2–SiO_2 and TiO_2–Al_2O_3 composites [12]; acidic supports involve silica–alumina or different kinds of zeolite and mesoporous materials [13]. Since TiO_2 supports have no pore system, their specific surface areas are very small compared to that of alumina, furthermore, the active anatase structure possesses only low thermal stability, which made TiO_2 support alone unsuitable for industrial applications [14]. But the TiO_2-Al_2O_3 oxide composites that were often composed of a heterogeneous mixture of the two oxides provided much higher specific surface areas and revealed a positive effect on tetralin conversion [15].

Acidic supports are not only to provide acidity but also to offer an ordered pore structure that facilitates high activity. Due to the high surface area of these mesoporous materials, high active phase loading is easy to be achieved [16]. The applications of mesoporous supports like MCM-41 and SBA-15 might conduce to improve the selectivity as their parallel pores might act as microreactors, in which the reactant and the intermediary products will be in the prolonged contact with the active phase [17].

In this paper, various Mo supported catalysts over γ-Al_2O_3 and two type mesoporous sieve supports and a mesoporous composite $MoSiO_x$ were prepared for diesel hydrotreating and were compared with a commercial catalyst.

2. Experimental

2.1. Feed properties

The feedstock was a 320 ppm sulphur diesel which was a blend of two commercial available diesels: a partially hydrotreated diesel from Fushun refinery and a catalytic cracking diesel from Shengli refinery in China. The properties of the diesel feedstock are shown in Table 1.

Table 1
Diesel feedstock properties

Properties	
Density at 20 °C (g/cm^3)	0.8195
Sulphur (ppm)	319.82
Distillation (°C)	
IBP	154
10%	218
30%	258.2
50%	290
70%	316.1
95%	365
FBP	450.8

2.2. Catalyst preparation

The γ-Al_2O_3 used in this study had a high surface area and large pore volume. Catalyst samples were prepared by impregnation of the γ-Al_2O_3 supports with aqueous solutions of ammonium heptamolybdate and/or nickel nitrate separately through incipient-wetness impregnation method, and the precursors were dispersed in an ultra-sonic unit for 30 min. The catalyst samples were dried in air for 8 h at 120 °C and calcined for 5 h at 550 °C. The active metal loadings of MoO_3 vary from 1 to 24 wt.%. These samples are labeled as: Cat 1–7 for MoO_3 content of 1, 4, 8, 12, 16, 20 and 24 wt.%. The bimetallic catalyst Cat_{NiMo} contains 16 wt.% MoO_3 and 3.5 wt.% of NiO. The catalysts were presulphided in a 2 wt.% CS_2 in cyclohexane stream for 4 h at 300 °C.

A mesoporous composite $MoSiO_x$ was prepared by the sol–gel process according to the following proportions of chemicals: 1 tetraethyl orthosilicate (TEOS):1 Mo:2.16 NaOH:0.13 cetyltrimethyl-ammonium bromide (CTMAB):107 H_2O:3.56 Acac. The sequence of preparation procedure were adding 1 mol/L NaOH solution, $(NH_4)_6Mo_7O_{24}{\cdot}4H_2O$, Acac, CTMAB and TEOS. The mixture was agitated for 3 h and aged for 7 days, then washed, filtered and calcined at 550 °C for 5 h. The MoO_3 content in the mesoporous material prepared by in situ synthesis in the strong caustic media reached 5 wt.%.

Two types of mesoporous sieves, MEM-1 and MEM-2 with different acidity were prepared by adding the grains of 5 g silica gel, 1 g sodium aluminate and 0.5 g sodium hydroxide into 2.23 g TEAOH solution at controlled pH value and mixed with 3.25 g PEG400 at 140 °C for 28 h. The resulting carriers were obtained after drying at 100 °C for 12 h and calcination at 550 °C for 5h. These carriers were supported with 3 wt.% NiO and 12 wt.% MoO_3.

2.3. Catalyst characterization

The specific surface area of catalyst samples was determined by the BET method. X-ray powder diffraction (XRD) profiles were recorded in an XRD-6000 X-ray diffractometer using Cu Kα radiation under 40 kV, 30 mA, scan range from 5 to 75° at a rate of 4° min^{-1} The IR spectra were taken within the range of 6000–400 cm^{-1} on an FTS-3000 spectrophotometer using 2 mg of the sample mixed with 200 mg of KBr, which was pressed into a transparent disc. The UV–vis diffuse reflectance spectra (DRS) experiments were performed on a Hitachi U-4100 UV–vis spectrophotometer with the integration sphere diffuse reflectance attachment. The powder samples were loaded in a transparent quartz cell and were measured in the region of 200–800 nm under ambient conditions. The standard support reflectance was used as the baseline for the corresponding catalyst measurement. FTIR spectra of adsorbed pyridine were recorded in order to evaluate the acidity of samples in BIO-RAD FTS3000 spectrophotometer with resolution of 4 cm^{-1}. The catalyst samples were made in the form of a self-supporting thin wafer, placed at the center of the cell vertical to the IR beam. Samples were pretreated in the infrared cell and fitted with greaseless stopcocks and KBr

windows, then the spectrum was scanned with an infrared spectrometer at speed of 20 scans/spectrum.

2.4. Catalytic activity

Catalyst activity test were performed in a JQ-II fixed-bed high-pressure micro-hydrotreating apparatus. Catalyst were presulphided at 350 °C for 4 h with a continuous stream of 3 wt.% CS_2/hexane solutions. After that, the diesel feedstock was fed continuously to the reactor. The experimental conditions are: total pressure, 5 MPa; reaction temperature, 350 °C; liquid hourly space velocity (LHSV), 1 h^{-1} and hydrogen-to-hydrocarbon ratio, 600 mL/mL. Reaction products were collected to determine the catalyst activities after 12 h feed on-stream.

The contents of sulphur in feed and products were measured with a PFPD detector in an ANTEK7000NS system, according to the ASTM 5463 method. The distribution of sulphur species was determined by GC–MS.

3. Results and discussion

3.1. Catalyst characterization

The textural properties and pore size distributions of catalysts are typically shown in Table 2 and Fig. 1, respectively. The catalysts include a commercial NiMo/γ-alumina catalyst (Com) with 2.7 wt.% NiO and 26.5 wt.% MoO_3, and a series of Mo supported catalysts (which have been labeled above).

Comparison with the pore size distributions of alumina-supported molybdenum (Mo) series catalysts and commercial alumina-supported NiMo catalyst in Table 2, the mesoporous γ-Al_2O_3 support exhibits higher surface area of 280 m^2/g and wider pore size of 12.3 nm, which result in high surface area and large pore size over Mo series catalysts, e.g. the surface area and the average pore size of Cat 6 are 239 m^2/g and 11.9 nm, but those of commercial catalyst are 155 m^2/g and 7.9 nm. As one of the Mo supported series catalysts, Cat 4 and Cat 7 also have the similar average pore sizes, but have different surface areas for different MoO_3 loading over γ-Al_2O_3 support (the Mo contents of Cat 4, Cat 6 and Cat 7 are 12, 20 and 24 wt.%), which indicate that the Mo Cat series catalysts and Cat_{NiMo} catalyst, supported on γ-Al_2O_3, have high surface area and large average pore size. It is well known that high surface area is adequate for dispersing metal to form active sites, while large pore diameter reduces the diffusion hindrance and promotes the contacts of reactant molecules with active sites on the catalyst surface.

Table 2
Catalyst textural properties

Catalysts	A_{BET} (m^2/g)	A_{micro} (m^2/g)	V_{BJH} (cm^3/g)	Average pore diameter (nm)
Cat 4	264	9	0.71	12.0
Cat 6	239	7	0.71	11.9
Cat 7	223	8	0.68	11.7
Com	155	0	0.30	7.9
$MoSiO_x$	~1000	0	1.50	3.7
MEM-1	189	128	0.19	4.0
MEM-2	236	163	0.21	3.6
γ-Al_2O_3	280	22	0.75	12.3

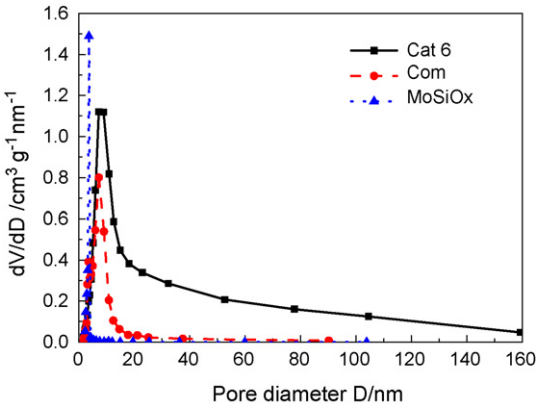

Fig. 1. Pore size distribution.

The typical pore size distributions of several catalysts in Fig. 1 show that Cat 6 catalyst, as a representative of Mo Cat series, possesses plenty of pores with different pore-sizes even as large as 100 nm that provide unblocked channels for reactant molecules with various sizes. The commercial catalyst has a symmetrical distribution around 7.9 nm in pore size and the mesoporous $MoSiO_x$ catalyst reveals a relatively uniform pore size of 3.7 nm, which maybe induces internal diffusion limitation of large size molecules.

Fig. 2 presents XRD patterns of Mo Cat series catalysts, indicating no apparent signals of MoO_3 crystal. This suggests that the dispersion of MoO_3 on catalyst was either relatively high or the crystallite size of MoO_3 was very small. Fig. 3 shows the low-angle XRD pattern (Fig. 3a) and wide-angle XRD pattern (Fig. 3b) of mesoporous $MoSiO_x$. In Fig. 3a, the very intense reflection peak at 1.96° (2θ) and the reflection line in the range of 3–3.75° (2θ) are characteristic of the mesoporous $MoSiO_x$ structure. The XRD pattern in Fig. 3b shows the spectrum of wider angle corresponding to 2θ from 5 to 75°, indicating no peak corresponding to ordered crystal. This suggests that the MoO_x was highly dispersed with particle size less than 40 Å which was beyond XRD detection limitation. The finely dispersed nanocrystalline MoO_x particles are believed to

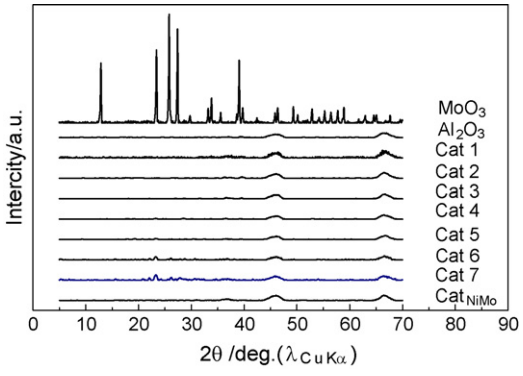

Fig. 2. XRD patterns of Mo Cat series catalysts.

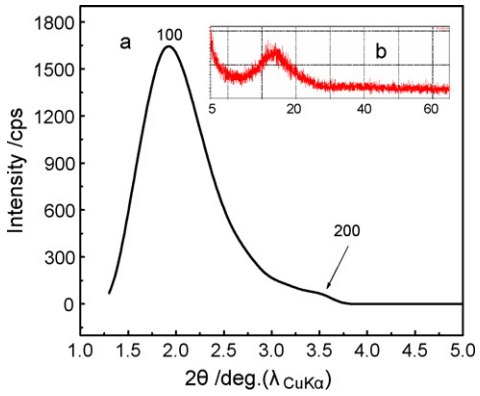

Fig. 3. (a) The low-angle and (b) wide-angle XRD patterns of $MoSiO_x$.

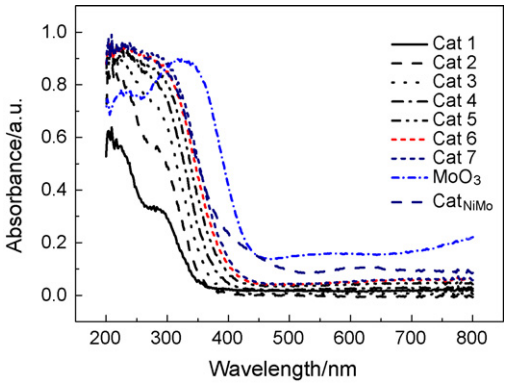

Fig. 5. UV–vis DR spectra of catalysts.

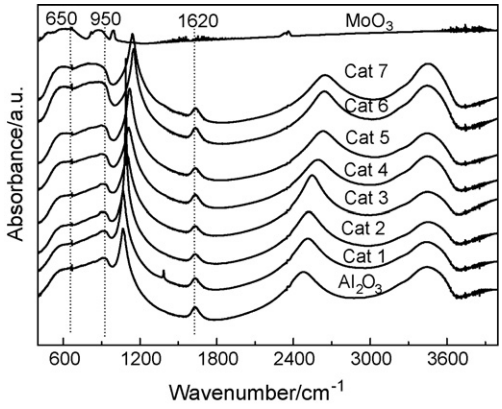

Fig. 4. FT-IR spectra of catalysts.

improve the catalyst activity, since the higher active surface with smaller size of active phase provides more effective contacts with the reactants [18–20].

FT-IR spectroscopy in Fig. 4 shows the surface compositions and structures of the Mo Cat series catalysts. The band at 950 cm^{-1} characterizes the stretching mode of terminal Mo=O bonds in molybdenum octahedral in polymeric molybdenum compounds (iso- and heteropolymolybdates). The band at 650 cm^{-1} ascribes to the characteristic bridged Mo–O–Mo bonds. The increased trend of band intensities between 600 and 950 cm^{-1} corresponds to an increase in Mo loading, suggesting the polymer formation of molybdenum-oxygen (MoO_x) species (clusters). The bands at 1620 and 3500 cm^{-1} indicate the deformation and stretch vibration of the O–H bonds. The high-intensity band at 1100 cm^{-1} is likely ascribed to the deformation vibration of the Al–OH bond [21,22].

The UV–vis DRS was applied to determine the structures of supported Mo catalysts in the 200–800 nm region. The DR spectra in Fig. 5 show that there is no typical signal of MoO_3 crystal existing in the catalyst surface which is consistent with the XRD analysis. When Mo loading is low, the Mo surface species are mostly Mo^{6+} over alumina support; with Mo loading increasing a few of low valence Mo species appear. The bands at 220–250 nm are commonly attributed to the tetrahedral molybdate, whereas the band at 320 nm is assigned to the Mo–O–Mo bridge bond of the octahedral coordination [23,24]. The band at 280 nm is assigned to monomer, dimer or polymerized molybdate species, but the assignment is not clear yet [25]. The broad band at 280–400 nm in Fig. 5 indicates that both the tetrahedral and octahedral molybdates can be present on the support. There were more tetrahedral species at low Mo loadings and more octahedral species at high Mo loadings. The red shift of the lowest energy transition absorption of molybdate indicates that the molybdate species formed larger clusters as Mo loading increased [26,27], but the active phase is still in high dispersion and there is no large size MoO_3 crystal over catalyst surface.

The IR spectra of the pyridine adsorbed on the various samples in the region 1700–1400 cm^{-1} are shown in Fig. 6. The bands at 1540 and 1450 cm^{-1} are related to the adsorption of the pyridine molecule on Brønsted acid sites and Lewis acid sites. Table 3 is the acid strength distributions of samples quantitatively calculated from IR results of pyridine adsorption at 200 and 350 °C, respectively, which recompile the

Table 3
Acidity of different catalysts

Sample	Concentration of acid sites (mmol/g_{cat})							
	Brønsted		Lewis		Total		*B/L*	
	250 °C	350 °C	250 °C	350 °C	250 °C	350 °C	250 °C	350 °C
Com	1.8	0.7	17.7	5.4	19.5	6.1	0.10	0.13
Cat 6	2.3	1.3	20.1	8.6	23.4	9.9	0.11	0.15
Cat_{NiMo}	4.2	3.4	24.7	13.8	28.9	17.2	0.17	0.25
MEM-1	5.4	1.0	30.9	14.6	36.3	15.6	0.17	0.07
MEM-2	3.7	1.0	20.7	10.2	24.4	11.2	0.18	0.10

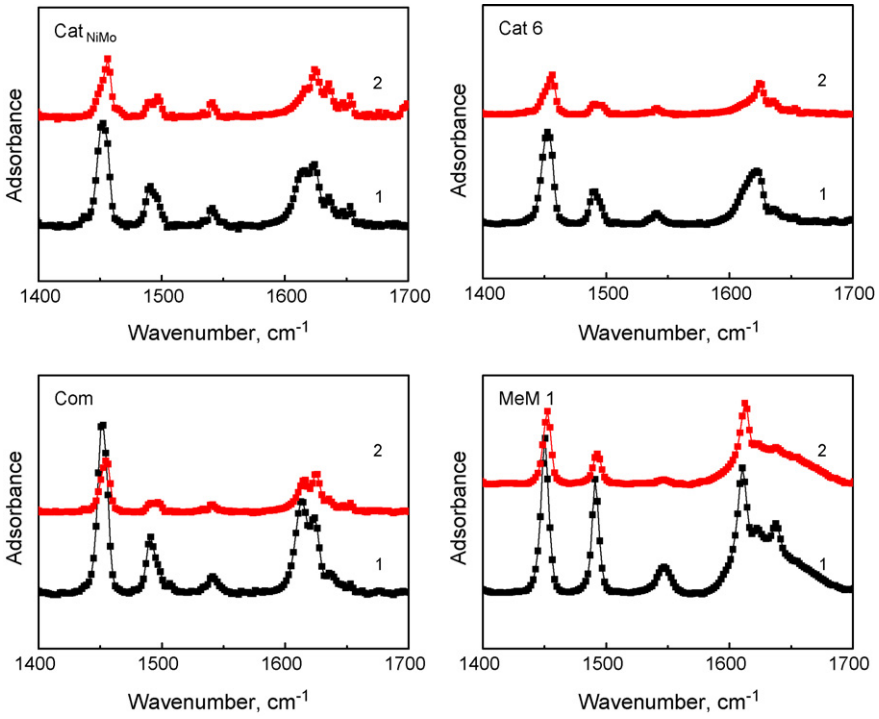

Fig. 6. IR spectra of the pyridine adsorbed on various catalysts at different temperatures: (1) 200 °C and (2) 350 °C.

concentrations of total acid sites, Brønsted, Lewis and *B*/*L* ratios of all catalysts.

From these data the *B*/*L* ratio follows the order: Cat_{NiMo} > MEM-2 > Cat 6 > MEM-1 > Com; the total acidity follows: MEM-1 > Cat_{NiMo} > MEM-2 > Cat 6 > Com. It is clear that Cat_{NiMo} exhibits the highest *B*/*L* ratio and the concentrations of Brønsted and Lewis acid sites keep relatively high level at these two thermal desorption temperature. The MEM-1 and MEM-2 catalysts give also high concentration of Brønsted acid sites and Lewis acid sites at low temperature, but the concentration of medium and strong Brønsted acid sites decline sharply. Compared with the commercial catalyst, catalysts Cat 6 and Cat_{NiMo} produce more Brønsted and Lewis acid sites, which should be of significance for hydrotreating applications.

3.2. Catalytic activity

Table 4 shows the HDS activities over various catalysts. The HDS efficiency data of the Mo supported series catalysts indicate that in the low Mo loading range, HDS activity of Mo Cat series catalysts increases with Mo loading, which may be enhanced not only by the increased dispersion of Mo but also by higher Brønsted acid sites concentration, until the Mo loading is as high as 20–24 wt.% of MoO_3. When MoO_3 loading is greater than 20 wt.%, the HDS efficiencys are above 95%, which are comparable to that of commercial catalyst. For the bimetallic Cat_{NiMo} catalyst, the sulphur content in the product is so low that it is below the detection limit of PFPD and GC–MS analyses, thus its HDS activity is near to 100% which is superior to that of commercial catalyst.

Since the total Mo content was only 5 wt.% incorporated into the framework of mesoporous $MoSiO_x$ catalyst, the HDS activity was as low as 80.6%. So the amounts of MoO_3 over the catalyst surface should be kept on a relatively high level for the future preparation.

Even though the meso-microporous composite molecular sieves carrier catalysts, MEM-1 and MEM-2 show high acidities as shown in Table 3, their HDS activities are much lower than that of other catalysts. That maybe due to the mesoporous material and molecular sieves having uniform pore distribution less than 4 nm (see Table 2 and Fig. 1), which restrict the internal diffusivity of reactant molecules in the pores of molecular sieves.

Table 5 compares the sulphur compounds in the feedstock and reaction products over various catalysts. Since the

Table 4
HDS efficiency over various catalysts at 350 °C, 5 MPa, 1 h^{-1} and 600 mL H_2/mL oil

Catalysts	Cat 1	Cat 3	Cat 4	Cat 6	Cat 7	Cat_{NiMo}	$MoSiO_x$	Com	MEM-1	MEM-2
MoO_3 (wt.%)	1	8	12	20	24	16	5	26	12	12
NiO (wt.%)						3.5		2.7	3	3
Sulphur in product (ppm)	124.9	25.1	26.4	16.0	15.5	–	61.9	17.5	36.7	71.0
HDS Conv. (%)	61.0	92.2	91.7	95.1	95.2	~100	80.6	94.5	88.5	77.8

Table 5
Comparison of product sulphur compounds with various catalysts at 350 °C, 5 MPa, 1 h^{-1} and 600 mL H_2/mL oil

	Sulphur contents (by GC–MS, ppm)						
	Feed	Cat 1	Cat 3	Cat 4	Cat 6	Cat 7	Cat_{NiMo}
BT	3.9	0	0	0	0	0	
C1-BT	34.6	2.4	0	0	0	0	
C2-BT	59.9	11.8	0.3	0	0	0	0
C3-BT	34.4	11.7	0.7	0.3	0	0	0
≥C4-BT	33.4	5.6	0	0	0	0	0
DBT	6.7	3.8	0	0	0	0	0
C1-DBT	23.3	15.9	5.8	0.7	0	0	0
C2-DBT	38.0	20.9	5.3	0.7	0.3	0.3	0
≥C3-DBT	39.0	25.5	6.2	0.8	0.7	0.3	0
Total	273.2	97.6	18.2	2.5	1.0	0.6	0

BT, benzothiophene; Ci-BT, alkyl-benzothiophene; DBT, dibenzothiophene; Ci-DBT, alkyl-dibenzothiophene.

feedstock was a blend of partially hydrotreated diesels from the commercial refineries, the sulphur compounds in the feedstock were primarily alkyl-benzothiophenes (alkyl-BT) and alkyl-dibenzothiophenes (alkyl-DBT). These refractory sulphur compounds needed to be decomposed in hydrotreating process. The percentages of alkyl-BT and alkyl-DBT over total sulphur content in feedstock are 51.9 and 33.4 wt.%, respectively. From the data in Table 5, the amounts of alkyl-BT and alkyl-DBT in the diesel products over the Mo series catalysts decreased greatly with increasing Mo loadings, e.g. for Cat 6 and Cat 7 the total sulphur are even near to trace amounts, which verify their good hydrogenation abilities in HDS reaction. As for the Cat_{NiMo} catalyst, no sulphur compounds is detected by PFPD and GC–MS methods, and it shows very high activity towards $\geq C_3$ DBT, which is consistent to the high surface area and large pore diameters of its γ-Al_2O_3 support. Therefore, comparing catalyst activities, Cat_{NiMo} catalyst is capable of producing ultra low sulphur diesel in order to meet the stringent fuel specifications.

4. Conclusions

The catalyst characterizations of BET, XRD, FT-IR, UV–vis DRS and FTIR pyridine adsorption shows that the existences of metal active component Mo in the supported catalysts are highly dispersed nano MoO_3 clusters which favors the HDS activity, and the Mo series catalysts have high surface areas and plenty of large pores propitious to the diffusions of reactant and product molecules.

HDS activity of Mo Cat series catalysts increases with Mo loading, which is enhanced not only by the increased dispersion of Mo but also by higher Brønsted acid sites concentration, until the Mo loading is as high as 20–24 wt.% of MoO_3. Cat_{NiMo} exhibits the highest *B*/*L* ratio and higher total concentrations of Brønsted acid sites and Lewis acid sites, and its HDS activity is superior to that of commercial catalyst (HDS efficiency for Com catalyst is 95 wt.%). As concerning the HDS of sulphur compounds it is found that synthesized Cat_{NiMo} catalyst shows very high activity towards $\geq C_3$ DBT, which is capable of producing a sulphur-free diesel.

The mesoporous $MoSiO_x$ catalyst shows a relatively low HDS activity as the MoO_3 loading is only 5 wt.%. The meso-microporous composite molecular sieves carrier catalysts, MEM-1 and MEM-2 show that the former has the highest total acidity, but their HDS activities are much lower than that of Mo Cat series for their typical pore diameter less than 4 nm.

Acknowledgements

This work was supported by NSFC project (No. 20406012), CNPC project (04A5050102 and 05E7019), the National Basic Research Program of China (No. 2004CB217806), and SKLHOP open project 2004–06 of China University of Petroleum (Beijing).

References

[1] D.D. Whitehurst, H. Farag, T. Nagamatsu, Catal. Today 45 (1998) 299.
[2] J.J. Lee, H. Kim, S.H. Moon, Appl. Catal. B 41 (2003) 171.
[3] J.W. Ward, in: G. Poncelet (Ed.), Preparation of Catalysts, Elsevier Science, Amsterdam, 1983, p. 212.
[4] J.V. Lauritsen, S. Helveg, E. Lagsgaard, J. Catal. 197 (2001) 1.
[5] D.R.M. Perez, T. Samuel, B. Gilles, C. Alejandra, Y.M. Jose, et al. J. Catal. 225 (2004) 288.
[6] H. Shimada, Catal. Today 86 (2003) 17.
[7] H. Topsøe, B.S. Clausen, F.E. Massoth, in: J.R. Anderson, M. Boudart (Eds.), Hydrotreating Catalysts, Catal. Science Technol., vol. 11, Springer, Berlin, 1996.
[8] P.T. Vasudevan, J.L.G. Fierro, Catal. Rev. Sci. Eng. 38 (1996) 161.
[9] D.D. Withehurst, T. Isoda, I. Mochida, Adv. Catal. 42 (1998) 345.
[10] C. Song, Catal. Today 86 (2003) 211.
[11] G. Murali Dhar, B.N. Srinivas, M.S. Rana, et al. Catal. Today 86 (2003) 45–60.
[12] S.K. Maity, J. Ancheyta, L. Soberanis, et al. Appl. Catal. A 244 (2003) 141.
[13] T. Klimova, E. Rodriguez, M. Martinez, et al. Microporous Mesoporous Mater. 44-45 (2001) 357.
[14] S. Yoshinaka, K. Segawa, Catal. Today 45 (1998) 293.
[15] M. Breysse, P. Afanasiev, C. Geantet, et al. Catal. Today 86 (2003) 5.
[16] C. Song, K.M. Reddy, Appl. Catal. A 176 (1999) 1.
[17] S. Dzwigaj, C. Louis, M. Breysse, et al. Appl. Catal. B 41 (2003) 181.
[18] H. Topsoe, B.S. Clausen, N. Topsoe, in: D.L. Trimm, S. Akashah, M. Absi Halabi (Eds.), Catalysts in Petroleum Refining, Stud. Surf. Sci. Catal., vol. 53, Elsevier, Amsterdam, 1990, p. 77.
[19] S.M.A.M. Bouwens, R. Prins, V.H.J. de Beer, J. Phys. Chem. 95 (1991) 123.
[20] R. Prins, in: G. Ertl, H. Knozinger, J. Weitkam (Eds.), Handbook of Heterogeneous Catalysis, VCH, Weinheim, 1908.
[21] R.G.V. Rama, S. Venkadesan, V. Saraswati, J. Mater. Sci. 111 (1989) 103.
[22] F.E. Massoth, Adv. Catal. 27, 283.
[23] T. Klimova, M. Calderón, J. Rańırez, Appl. Catal. A 240 (2003) 29.
[24] M. Cheng, F. Kumata, T. Saito, T. Komatsu, Appl. Catal. A 183 (1999) 199.
[25] Y. Iwasawa, M. Yamagishi, J. Catal. 82 (1983) 373.
[26] G. Xiong, C. Li, Z. Feng, J. Catal. 186 (1999) 234.
[27] G. Xiong, Z. Feng, J. Li, et al. J. Phys. Chem. 104 (2000) 3581.